

# A non factorized calculation of the process ${}^3\text{He}(e, e'p){}^2\text{H}$ at medium energies

C. Ciofi degli Atti and L.P. Kaptari\*

*Department of Physics, University of Perugia and Istituto Nazionale di Fisica Nucleare,  
Sezione di Perugia, Via A. Pascoli, I-06123, Italy*

(Dated: March 22, 2022)

## Abstract

The exclusive process  ${}^3\text{He}(e, e'p){}^2\text{H}$  has been analyzed using realistic few-body wave functions corresponding to the  $AV18$  interaction and treating the final state interaction (FSI) within the Eikonal Approximation to describe the multiple rescattering of the struck nucleon with the nucleons of the spectator two-nucleon system. Calculations have been performed in momentum space so that the nucleon electromagnetic current could be left in the fully covariant form avoiding by this way non relativistic reductions and the factorization approximation. The results of calculations, which are compared with recent JLab experimental data, show that the left-right asymmetry exhibit a clear dependence upon the multiple scattering in the final state and demonstrate the breaking down of the factorization approximation at  $\phi = 0$  i.e. for "negative" and large  $\geq 300\text{MeV}/c$  values of the missing momentum.

---

\*On leave from Bogoliubov Lab. Theor. Phys.,141980, JINR, Dubna, Russia

## I. INTRODUCTION

Recent experimental data from Jlab on exclusive electro-disintegration of  ${}^3\text{He}$  [1, 2] are at present the object of intense theoretical activity (see [3, 4, 5, 6, 7, 8] and References therein). In Refs. [3, 4] the 2- and 3-body break up channels have been calculated within an approach where:

i) initial state correlations (ISC) have been taken care of by the use of the status-of-the-art few-body wave functions [9] corresponding to the *AV18* interaction [10];

ii) final state interactions (FSI) have been treated by a Generalized Eikonal Approximation [11], which represents an extended Glauber approach (GA) based upon the evaluation of the relevant Feynman diagrams that describe the rescattering of the struck nucleon in the final state, in analogy with the Feynman diagrammatic approach developed for the treatment of elastic hadron-nucleus scattering [12, 13].

In [3, 4] theoretical calculations have been compared with preliminary Jlab data covering a region of "right " ( $\phi = \pi$ ,  $\phi$  being the azimuthal angle of the detected proton, with respect to the momentum transfers  $\mathbf{q}$ ) values of the missing momentum  $p_m \leq 1.1 \text{ GeV}/c$  and missing energy  $E_m \leq 100 \text{ MeV}$ . Published data [1], however, cover both the right ( $\phi = \pi$  and  $p_m \leq 1.1 \text{ GeV}/c$ ) and left ( $\phi = 0$  and  $p_m \leq 0.7 \text{ GeV}/c$ ) values of the missing momentum which have not been considered in [3, 4]. It is the aim of this paper to analyze the process in the entire kinematical range improving, at the same time, our theoretical approach. As a matter of fact, previous calculations of ours, which took into account the Final State Interaction (FSI), have been based upon the factorization approximation which, as is well known, leads to a form of the cross section in terms of a product of two factors, one describing the electromagnetic electron-nucleon interaction, the other depending upon nuclear structure and the strong interaction of nucleons in the final state. The factorization form is exactly satisfied in the Plane Wave Impulse Approximation (PWIA), but it is however violated in presence of FSI effects.

Within the factorization approximation, the  $\phi$ -dependence of the cross section is only due to the  $\phi$ -dependence of the elementary cross section for electron scattering off a moving nucleon [14]. Such a dependence is a very mild one and the recent data[1] on the left-right asymmetry unambiguously demonstrates that at  $p_m \geq 0.35 \text{ GeV}/c$ , the cross section at  $\phi = 0$  appreciably differs from the one at  $\phi = \pi$ . This, as is well known, is clear evidence

that the factorization approximation cannot explain the left-right asymmetry. Several non factorized calculations appeared in the past. It should however be pointed out that most of them worked in configuration space, and in so doing the on mass shell current operator, which is exactly defined in momentum space, had to be reduced non relativistically by different prescriptions. In the present paper we extend our approach by releasing the factorization approximation and, at the same time, avoiding non relativistic reductions by directly performing our calculations in momentum space, treating the full current operator without any approximation. The  ${}^3\text{He}$  wave function of the Pisa group [9], corresponding to the AV18 interaction [10] is used in the calculations. We do not consider, for the time being, Meson Exchange Currents (MEC),  $\Delta$ -Isobar Configurations, and similar effects, which have been the object of intensive theoretical studies in  $A(e, e'p)B$  processes off both few-body systems (see e.g. [8, 15]) and complex nuclei (see e.g. [16] and References therein quoted). We fully concentrate on the effects of the FSI, treating the initial and final state correlations, the Final State Interaction and the current operator within a parameter-free self-consistent approach.

Recently [5], the  ${}^3\text{He}(e, e'p)^2\text{H}$  process and the left-right asymmetry have been calculated within a non factorized GA approach, considering also the effects of MEC, adopting a non relativistic form for the nucleon electromagnetic current operator.

## II. THE PROCESS ${}^3\text{He}(e, e'p)^2\text{H}$ . BASIC FORMULISM

We will consider the process

$$e + A = e' + p + (A - 1)_f \quad (1)$$

where the relevant kinematical variables are defined as follows:  $k = (E, \underline{k})$  and  $k' = (E', \underline{k}')$ , are electron momenta before and after interaction,  $P_A = (E_A, \underline{P}_A)$  is the momentum of the target nucleus,  $p_1 = (\sqrt{\underline{p}_1^2 + m_N^2}, \underline{p}_1)$  and  $P_{A-1} = (\sqrt{\underline{P}_{A-1}^2 + (M_{A-1}^f)^2}, \underline{P}_{A-1})$ , are the momenta of the final proton and the final  $A - 1$  system,  $m_N$  is the nucleon mass,  $M_{A-1}^f = M_{A-1} + E_{A-1}^f$ , where  $E_{A-1}^f$  is the *intrinsic* excitation energy of the  $A - 1$  system. The 4-momentum transfer is  $Q^2 \equiv -q^2 = (\nu, \mathbf{q})$ . The relevant quantities which characterize the process are the *missing momentum*  $\underline{p}_m$  (i.e. the total momentum of the  $A - 1$  system), and

the *missing energy*  $E_m$  defined, respectively, by

$$\underline{p}_m = \underline{q} - \underline{p}_1 \quad E_m = \sqrt{P_{A-1}^2} + m_N - M_A = E_{min} + E_{A-1}^f. \quad (2)$$

where  $E_{min} = M_{A-1} + m_N - M_A = |E_A| - |E_{A-1}|$  is the threshold energy for the two-body break-up (2bbu) channel. The differential cross section for the exclusive process has the following form

$$\frac{d^6\sigma}{d\Omega' dE' d^3\underline{p}_m} = \sigma_{Mott} \sum_i V_i W_i^A(\nu, Q^2, \underline{p}_m, E_m), \quad (3)$$

where  $i \equiv \{L, T, TL, TT\}$ , and  $V_L, V_T, V_{TL}$ , and  $V_{TT}$  are well-known kinematical factors [17]; the nuclear response functions  $W_i^A$  are

$$\begin{aligned} W_L &= \left[ \frac{\mathbf{q}^2}{Q^2} W_{00} \right]; & W_{TL} \cos \phi &= \frac{|\mathbf{q}|}{\sqrt{Q^2}} [2\Re(W_{01} - W_{0-1})]; \\ W_T &= [W_{11} + W_{-1-1}]; & W_{TT} \cos 2\phi &= (2\Re(W_{1-1})), \end{aligned} \quad (4)$$

with

$$W_{\lambda\lambda'} = (-1)^{\lambda+\lambda'} \varepsilon_\lambda^\mu W_{\mu\nu} \varepsilon_{\lambda'}^{*\nu} \quad (5)$$

$\varepsilon_\lambda$  being the polarization vectors of the virtual photon. The hadronic tensor  $W_{\mu\nu}^A$  is defined as follows

$$\begin{aligned} W_{\mu\nu}^A &= \frac{1}{4\pi M_A} \overline{\sum_{\alpha_A}} \sum_{\alpha_{A-1}, \alpha_N} (2\pi)^4 \delta^{(4)}(P_A + q - P_{A-1} - p_1) \times \\ &\times \langle \alpha_A \underline{P}_A | \hat{J}_\mu^A(0) | \alpha_N \underline{p}_1, \alpha_{A-1} \underline{P}_{A-1} E_{A-1}^f \rangle \langle E_{A-1}^f \underline{P}_{A-1} \alpha_{A-1}, \underline{p}_1 \alpha_N | \hat{J}_\nu^A(0) | \alpha_A \underline{P}_A \rangle, \end{aligned} \quad (6)$$

where  $\alpha_i$  denotes the set of discrete quantum numbers of the systems  $A$ ,  $A-1$  and the nucleon  $N$  with momentum  $\underline{p}_1$ . In Eq. (6) the vector  $|\alpha_N \underline{p}_1, \alpha_{A-1} \underline{P}_{A-1} E_{A-1}^f\rangle$  consists asymptotically of the nucleon  $N$  and the nucleus  $A-1$ , with momentum  $\underline{P}_{A-1}$  and intrinsic excitation energy  $E_{A-1}^f$ . The evaluation of the nuclear response functions  $W_i^A$  requires the knowledge of both the nuclear vectors  $|\alpha_A \underline{P}_A\rangle$  and  $|\alpha_N \underline{p}_1, \alpha_{A-1} \underline{P}_{A-1} E_{A-1}^f\rangle$ , and the nuclear current operators  $\hat{J}_\mu^A(0)$ . In the present paper we describe the two- and three-body ground states in terms of realistic wave functions generated by modern two-body interactions [9], and treat the final state interaction by a diagrammatic approach of the elastic rescattering of the struck nucleon with the nucleons of the  $A-1$  system [3, 4, 18]. We consider the interaction of

the incoming virtual photon  $\gamma^*$  with a bound nucleon (the active nucleon) of low virtuality ( $p^2 \sim m_N^2$ ) in the quasi-elastic kinematics i.e. corresponding to  $x \equiv Q^2/2m_N\nu \sim 1$ . In the quasi-elastic kinematics, the virtuality of the struck nucleon after  $\gamma^*$ -absorption is also rather low and, provided  $\underline{p}_1$  is sufficiently high, nucleon rescattering with the "spectator"  $A-1$  can be described to a large extent in terms of multiple elastic scattering processes in the eikonal approximation [3, 4, 18]. It should be pointed out that even within such an approximation one encounters problems in treating the operator of the electromagnetic current for off-mass shell nucleons. Up to now most approaches to the process (1) for complex nuclei, were based upon a non relativistic reduction of the on mass-shell nucleon current operator  $\hat{j}_\mu$  (the Foldy-Wouthuysen transformation) with subsequent, non relativistic, evaluations of matrix elements in co-ordinate space. In principle, the non relativistic reduction can be avoided by using the fully covariant expressions for the current operator  $\hat{j}_\mu$  within the factorization approximation (FA) or by performing calculations in momentum space. In latter case, calculations for complex nuclei in momentum space are hindered by the fact that realistic nuclear wave functions are obtained in co-ordinate space. As for the factorization approximation, it should be considered it not only guarantees that relativistic kinematics can be treated correctly, which is a prerequisite at high energies, but it also provides in various instances a satisfactory agreement with experimental data [4]. However, the inadequacies of the FA clearly manifest themselves in the calculation of specific quantities such as, for example, the left-right asymmetry with respect to the azimuthal angle  $\phi$ : if factorization holds, this quantity must precisely follow the well known behavior of the corresponding asymmetry in the electron-nucleon elastic scattering [14] so that deviations from such a behavior would represent a stringent evidence of the breaking down of the FA.

In this paper the results of calculations of the left-right asymmetry of the process  ${}^3\text{He}(e, e'p){}^2\text{H}$  obtained in the momentum space using realistic wave functions will be presented.

### A. The Final state interaction

In co-ordinate space the initial and final states of the process under consideration have the following form

$$\Phi_{3\text{He}}(\mathbf{r}_1, \mathbf{r}_2, \mathbf{r}_3) = \hat{\mathcal{A}}e^{i\mathbf{P}\mathbf{R}}\Psi_3(\boldsymbol{\rho}, \mathbf{r}),$$

$$\Phi_f^*(\mathbf{r}_1, \mathbf{r}_2, \mathbf{r}_3) = \hat{\mathcal{A}}S(\mathbf{r}_1, \mathbf{r}_2, \mathbf{r}_3)e^{-i\mathbf{p}'\mathbf{r}_1}e^{-i\mathbf{P}_D\mathbf{R}_D}\Psi_D^*(\mathbf{r}) \quad (7)$$

where  $\hat{\mathcal{A}}$  denotes a proper antisymmetrization operator and the  $S$ - matrix describing the final state interaction of nucleons within the eikonal approximation is

$$S(\mathbf{r}_1, \mathbf{r}_2, \mathbf{r}_3) = \prod_{j=2}^3 \left[ 1 - \theta(\mathbf{r}_{j\parallel} - \mathbf{r}_{1\parallel}) \Gamma(\mathbf{r}_{j\perp} - \mathbf{r}_{1\perp}) \right], \quad (8)$$

where the profile-function  $\Gamma(\mathbf{r}_\perp)$  is defined as

$$\Gamma(\mathbf{r}_\perp) = \frac{1}{2\pi i k^*} \int d^2\boldsymbol{\kappa}_\perp f_{NN}(\boldsymbol{\kappa}_\perp) e^{-i\boldsymbol{\kappa}_\perp \mathbf{r}_\perp} \quad (9)$$

and  $\boldsymbol{\rho}$ ,  $\mathbf{r}$  and  $\mathbf{R}$  are three-body Jacobi co-ordinates. In Eq. (9)  $f_{NN}(\boldsymbol{\kappa})$  is the elastic scattering amplitude of two nucleons with center-of-mass momentum  $k^*$ . By approximating the nuclear electromagnetic current operator with a sum of nucleonic currents  $\hat{j}_\mu(i)$  and supposing that the virtual photon interacts with the nucleon "1", one has

$$J_\mu^A = \int \prod d\mathbf{r}_i \Phi_f^*(\mathbf{r}_1, \mathbf{r}_2, \mathbf{r}_3) j_\mu(1) e^{-i\mathbf{q}\mathbf{r}_1} \Phi_{3He}(\mathbf{r}_1, \mathbf{r}_2, \mathbf{r}_3). \quad (10)$$

In what follows we consider the reaction (1) at relatively large (few  $GeV/c$ ) momentum transfers, which implies large relative momenta of the particles in the final states. This allows one to safely neglect the spin-flip terms in the  $NN$  amplitude considering only its central part. Then the matrix element (10) can be re-written in the momentum space as follows

$$J_\mu^A = \sum_\lambda \int \frac{d^3p}{(2\pi)^3} \frac{d^3\kappa}{(2\pi)^3} S(\mathbf{p}, \boldsymbol{\kappa}) \langle s_f | j_\mu(\boldsymbol{\kappa} - \mathbf{p}_m; \mathbf{q}) | \lambda \rangle \mathcal{O}(\mathbf{p}_m - \boldsymbol{\kappa}, \mathbf{p}; \mathcal{M}_3, \mathcal{M}_2, \lambda), \quad (11)$$

where the overlap integral  $\mathcal{O}(\mathbf{p}_m - \boldsymbol{\kappa}, \mathbf{p}; \mathcal{M}_3, \mathcal{M}_2, \lambda)$  is defined by

$$\mathcal{O}(\mathbf{p}_m - \boldsymbol{\kappa}, \mathbf{p}; \mathcal{M}_3, \mathcal{M}_2, \lambda) = \int d\boldsymbol{\rho} d\mathbf{r} e^{i(\mathbf{p}_m - \boldsymbol{\kappa})\boldsymbol{\rho}} e^{i\mathbf{P}\mathbf{r}/2} \Psi_3(\boldsymbol{\rho}, \mathbf{r}) \Psi_D^*(\mathbf{r}) \chi_{\frac{1}{2}\lambda}^\dagger \quad (12)$$

and the Fourier-transform of the eikonal  $S$ -matrix is

$$S(\mathbf{p}, \boldsymbol{\kappa}) = \int d\mathbf{r} d\boldsymbol{\rho} e^{-i\mathbf{P}\mathbf{r}} e^{i\boldsymbol{\kappa}\boldsymbol{\rho}} S(\boldsymbol{\rho}, \mathbf{r}). \quad (13)$$

The quantities  $\mathcal{M}_3$ ,  $\mathcal{M}_2$  and  $s_f$  represent the projections of the angular momentum of  ${}^3He$ , the deuteron and the final proton, respectively, and  $\lambda$  denotes the spin projection of the proton before the absorption of the virtual photon.

By considering different terms in the  $S$ -matrix (8), we are in the position to calculate different contributions (PWIA and single and double rescattering) in the nuclear matrix elements  $J_\mu^A$ , eq. (10), and in the response functions  $W_i$ , eq. (4).

### 1. *The PWIA*

In absence of FSI the  $S$ -matrix (8) in co-ordinate space is  $S(\mathbf{r}_1, \mathbf{r}_2, \mathbf{r}_3) = 1$  and, correspondingly,  $S(\mathbf{p}, \boldsymbol{\kappa}) = (2\pi)^6 \delta^{(3)}(\mathbf{p}) \delta^{(3)}(\boldsymbol{\kappa})$ . This allows one to recover the well-known expression for the electromagnetic current (10) in terms of the Fourier transform of an overlap integral of the wave functions in co-ordinate space

$$J_\mu^A(PWIA) = \sum_\lambda \langle s_f | j_\mu(-\mathbf{p}_m; \mathbf{q}) | \lambda \rangle \int d\rho e^{i\mathbf{p}_m \rho} \int d\mathbf{r} \Psi_{\mathcal{M}_3}(\boldsymbol{\rho}, \mathbf{r}) \Psi_{\mathcal{M}_2}^*(\mathbf{r}) \chi_{\frac{1}{2}\lambda}^\dagger. \quad (14)$$

Equation (14) corresponds exactly to the Feynman diagram shown in Fig. 1. Note that the square of the matrix element (14), averaged over initial ( $\mathcal{M}_3$ ) and summed over final ( $\mathcal{M}_2$  and  $s_f$ ) spin projections, is diagonal with respect to the summation indices  $\lambda, \lambda'$  (see, e.g., Ref. [3]), so that in the response functions and, consequently, the cross section, factorize in the well known form in terms of the familiar spectral function [?] and the electron-nucleon cross section,  $\sigma_{eN}$  [14].

### 2. *Single rescattering.*

The corresponding part of the  $S$ -matrix for the single rescattering process is

$$S(\mathbf{p}, \boldsymbol{\Delta}) = -\frac{(2\pi)^4 f_{NN}(\boldsymbol{\Delta}_\perp)}{k^* \boldsymbol{\Delta}_\parallel - i\varepsilon} \left[ \delta\left(\mathbf{p} - \frac{\boldsymbol{\Delta}}{2}\right) + \delta\left(\mathbf{p} + \frac{\boldsymbol{\Delta}}{2}\right) \right], \quad (15)$$

which leads to

$$J_\mu^A(1) = \sum_\lambda \int \frac{d\boldsymbol{\Delta}}{(2\pi)^2 k^*} \langle s_f | j_\mu(\mathbf{k}_1; \mathbf{q}) | \lambda \rangle \frac{f_{NN}(\boldsymbol{\Delta}_\perp)}{\boldsymbol{\Delta}_\parallel - i\varepsilon} \times [\mathcal{O}(-\mathbf{k}_1, \boldsymbol{\Delta}/2; \mathcal{M}_3, \mathcal{M}_2, \lambda) + \mathcal{O}(-\mathbf{k}_1, -\boldsymbol{\Delta}/2; \mathcal{M}_3, \mathcal{M}_2, \lambda)], \quad (16)$$

where  $\mathbf{k}_1$  is the momentum of the proton before  $\gamma^*$  absorption,  $\mathbf{k}_1 = \boldsymbol{\Delta} - \mathbf{p}_m$ , and  $\boldsymbol{\Delta}$  is the momentum transfer in the  $NN$  interaction. The corresponding Feynman diagram is depicted in Fig. 2. The longitudinal part of the nucleon propagator can be computed using the relation

$$\frac{1}{\boldsymbol{\Delta}_\parallel \pm i\varepsilon} = \mp i\pi \delta(\boldsymbol{\Delta}_\parallel) + P.V. \frac{1}{\boldsymbol{\Delta}_\parallel}. \quad (17)$$

It should be pointed out that in the eikonal approximation the trajectory of the fast nucleon is a straight line so that all the "longitudinal" and "perpendicular" components are defined in correspondence to this trajectory, i.e., the  $z$  axis in our case has to be directed along the momentum of the detected fast proton. It can also be seen that since the argument of the nucleonic current  $\langle s_f | j_\mu(\mathbf{k}_1; \mathbf{q}) | \lambda \rangle$  is related to the integration variable  $\Delta$ , the factorization form is no longer fulfilled. However, as shown in Ref. [3], if in the integral (11) the longitudinal part can be neglected, the factorization form can be approximately recovered.

In actual calculations the elastic amplitude  $f_{NN}$  is usually parametrized in the following form

$$f_{NN}(\Delta_\perp) = k^* \frac{\sigma^{tot}(i + \alpha)}{4\pi} e^{-b^2 \Delta_\perp^2 / 2}, \quad (18)$$

where the slope parameter  $b$ , the total nucleon-nucleon cross section  $\sigma^{tot}$  and the ratio  $\alpha$  of the real to the imaginary parts of the forward scattering amplitude, are taken from experimental data.

### 3. Double rescattering.

In the same manner the double rescattering  $S$ -matrix can be obtained in the following form

$$S(\mathbf{p}, \boldsymbol{\kappa}) = -\frac{(2\pi)^2}{k_1^* k_2^*} \int d\Delta_1 d\Delta_2 \frac{f_{NN}(\Delta_{1\perp}) f_{NN}(\Delta_{1\perp})}{(\Delta_{1\parallel} + i\varepsilon)(\Delta_{2\parallel} + i\varepsilon)} \delta\left(\mathbf{p} + \frac{\Delta_1 - \Delta_2}{2}\right) \delta(\boldsymbol{\kappa} + \Delta_1 + \Delta_2) \quad (19)$$

and, correspondingly, for the electromagnetic current one has

$$J_\mu^{A(2)} = \frac{1}{(2\pi)^4 k_1^* k_2^*} \sum_\lambda \int d\Delta_1 d\Delta_2 \frac{f_{NN}(\Delta_{1\perp}) f_{NN}(\Delta_{1\perp})}{(\Delta_{1\parallel} + i\varepsilon)(\Delta_{2\parallel} + i\varepsilon)} \times \langle s_f | j_\mu(\mathbf{k}_1; \mathbf{q}) | \lambda \rangle \mathcal{O}(-\mathbf{k}_1, (\Delta_1 - \Delta_2)/2; \mathcal{M}_3, \mathcal{M}_2, \lambda), \quad (20)$$

where now the proton momentum before interaction is  $\mathbf{k}_1 = \Delta_1 + \Delta_2 - \mathbf{p}_m$ . As in the previous case,  $\Delta_{1,2}$  are the momentum transfers in  $NN$  rescattering, as depicted in Fig. 3.

It can be seen from Eqs. (11) and (20) that the matrix element of the nucleon current operator  $\langle s_f | j_\mu(\mathbf{k}_1; \mathbf{q}) | \lambda \rangle$  is evaluated in momentum space. In the case of on-mass-shell nucleons the corresponding expression is



$$\langle s_f | j_\mu(\mathbf{k}_1; \mathbf{q}) | \lambda \rangle = \bar{u}(\mathbf{k}_1 + \mathbf{q}, s_f) \left[ \gamma_\mu F_1(Q^2) + i \frac{\sigma_{\mu\nu} q^\nu}{2m_N} F_2(Q^2) \right] u(\mathbf{k}_1, \lambda), \quad (21)$$

or, due to the Gordon identity,

$$\langle s_f | J_\mu(\mathbf{k}_1, \mathbf{q}) | \lambda \rangle = \bar{u}(\mathbf{k}_1 + \mathbf{q}, s_f) \left[ \gamma_\mu \left( F_1(Q^2) + F_2(Q^2) \right) - (2k_1 + q)_\mu F_2(Q^2) \right] u(\mathbf{k}_1, \lambda), \quad (22)$$

where  $F_{1,2}(Q^2)$  are the Dirac and Pauli nucleon form factors. Eqs. (21) and (22) for on mass shell nucleons are completely equivalent, however for the off mass shell case they could be rather different, for, in this case the Gordon identity does not hold. This leads to some arbitrariness and discussions about the actual choice of the nucleon current. In our calculations, following the de Forest prescription [14], we adopt the nucleonic current in form of Eq. (22), usually referred to as the "CC1" prescription.

### III. RESULTS OF CALCULATIONS

We have used the described formalism to calculate the cross sections of the processes (1). All two- and three-body wave functions were taken to be solutions of the non relativistic Schrödinger equation with the AV18 potential Ref. [9]. Calculations have been performed in PWIA and including the full rescattering within the eikonal approximation corresponding to the diagrams shown in Figs. 1-3.

The results of our calculations are shown in in Fig. 4 where they are compared with recent experimental data [1] corresponding to  $\phi = 0$  ( negative values of the missing momentum) and  $\phi = \pi$  (positive values of the missing momentum). The relevant kinematical variables in the experiment were  $|\underline{q}| = 1.5 \text{ GeV}/c$ ,  $\nu = 0.84 \text{ GeV}$ ,  $Q^2 = 1.55 (\text{GeV}/c)^2$ , and  $x \approx 1$ . In PWIA the cross section is directly proportional to the two-body spectral function of  ${}^3\text{He}$ . It can be seen that up to  $|\underline{p}_m| \sim 400 \text{ MeV}/c$ , PWIA and FSI results are almost the same and fairly well agree with the experimental data, which means that the 2bbu process  ${}^3\text{He}(e, e'p)^2\text{H}$  does provide information on the two-body spectral function; on the contrary, at larger values of  $|\underline{p}_m| \geq 400 \text{ MeV}/c$  the PWIA appreciably underestimates the experimental data. It is however very gratifying to see that when FSI is taken into account,

the disagreement is completely removed and an overall good agreement between theoretical predictions and experimental data is obtained. It should be pointed out that at large missing momenta the experimental data shown in Fig. 4 correspond to the perpendicular kinematics, when the deuteron momentum is always almost perpendicular to the momentum of the final proton; in such a kinematics the effects from FSI are maximized, whereas in the so-called parallel kinematics, they are minimized (see, e.g. [11], [20], [21]).

Fig. 4 shows, however, that in some regions quantitative disagreements with data still exist. Particularly worth being mentioned is the disagreement in the region around  $|\underline{p}_m| \simeq 0.6 - 0.65 \text{ GeV}/c$  at  $\phi = 0$ . Other possible mechanisms in this kinematical range (MEC,  $\Delta$  [5, 6, 7, 8]) which could remove this disagreement will be the object of future investigations.

We would like to stress, that in our calculations no approximations have been made in the evaluation of the single and double scattering contributions to the FSI: proper intrinsic coordinates have been used and the energy dependence of the profile function has been taken into account in the properly chosen CM system of the interacting pair. Note also, that the numerical values of the parameters are exactly the same for the left and right shoulders in the Fig. 4. The obtained results are clear evidence that the difference in the "left" and "right" cross sections has a dynamical origin entirely governed by FSI effects.

The "left-right" asymmetry is defined as follows

$$A_{TL} = \frac{d\sigma(\phi = 0^\circ) - d\sigma(\phi = 180^\circ)}{d\sigma(\phi = 0^\circ) + d\sigma(\phi = 180^\circ)}. \quad (23)$$

It can be seen from Eqs. (4) that the numerator in (23) is proportional to  $W_{TL}$ , whereas the denominator does not contain  $W_{TL}$  at all, i.e. the  $A_{TL}$  is a measure of the weight of the transversal-longitudinal components in the cross section, relative to the other responses. For the elementary  $eN$  cross section the behavior of the asymmetry  $A_{TL}$  is known to be a negative and decreasing function of the missing momentum [14]. It is clear that in the PWIA and within the FA the asymmetry (23) for the process (1) must be exactly the same as in the  $eN$  case. In Fig. 5 the asymmetry  $A_{TL}$  for the process (1) computed within the present approach is shown together with the available experimental data [1]. The dot-dashed line correspond to the PWIA, the dashed line includes single rescattering FSI, and, eventually, the solid line includes the full FSI. It can be seen that at  $p_m \leq 250 \text{ MeV}/c$  the PWIA result is in good agreement with the experimental data. However with increasing  $p_m$  the disagreement of the experimental data with the PWIA predictions appreciably increases. An interesting

observation can be made from an inspection of the behavior of the asymmetry  $A_{TL}$  in the region of  $p_m$  corresponding to the interference between different terms of the rescattering  $S$ -matrix (cf. Fig. 4). As a matter of fact, it can be seen that in this region the shape of the asymmetry, which strongly depends upon the value of the missing momentum, exhibiting a behaviour reflecting single and double rescattering in the final states. The change of slopes of the experimental data reflecting the multiple scattering structure has already been pointed out in Ref. [4]. It is also interesting to note that, as in the case of other calculations [5], the theoretical asymmetry does not agree with the experimental data. It should be noted, however, that for values of  $p_m$  up to  $p_m \sim 650 MeV/c$  the asymmetry is rather small  $\sim 0 - 20\%$ , i.e. the contribution of the response function  $W_{TL}$  to the total cross section is much smaller in comparison to other three responses, cf. Ref. [22]. Correspondingly, at high values of the missing momentum the analysis of the asymmetry  $A_{TL}$  does not allow one to draw definite conclusions about the limits of validity of the FA. For such a reason, let us define another quantity, which "amplifies" the limits of validity of the FA, namely following Ulmer et al. [23], we consider the so-called reduced cross section  $d\sigma_{red}$  defined by the ratio of the cross section (Eq. (3)) to the electron nucleon "CC1" cross section [14], i.e.

$$d\sigma_{red} = \frac{1}{\sigma_{cc1}} \frac{d^6\sigma}{d\Omega' dE' d^3\mathbf{p}_m}. \quad (24)$$

Then the deviation of the ratio

$$R = \frac{d\sigma^{red.}(\phi = 0)}{d\sigma^{red.}(\phi = \pi)} \quad (25)$$

from unity would be an indication of the breaking down of the FA. In Fig. 5 the ratio (25) calculated within the present approach is compared together with the corresponding experimental quantity, obtained from data [1]. It can be seen that up to values of  $p_m \sim 0.3 GeV/c$  the FA holds for both,  $\phi = 0$  and  $\phi = \pi$  (cf. also the PWIA results in Fig. 4). At larger values of  $p_m$  the ratio (25) is larger than one, with a tendency to remain constant as  $p_m$  increases.

#### IV. SUMMARY AND CONCLUSIONS

We have calculated in momentum space the cross section of the processes  ${}^3He(e, e'p){}^2H$ , using realistic ground state two- and three-body wave functions and treating the FSI of the

struck nucleon with the spectators within the eikonal approximation. The method we have used is a very transparent and parameter free one: it is based upon Eqs. (11), (12), and (22), which only require the knowledge of the nuclear wave functions, since the FSI factor is fixed directly by NN scattering data. At the same time, calculations are very involved mainly because of the complex structure of the wave function of Ref. [9], which has to be firstly transformed to momentum space and then used in calculations of multidimensional integrals, including also the computations of Principal Values (see eq. (17)) together with the Dirac algebra for the electromagnetic current (22). Several aspects and results of our approach deserve the following comments:

1. our calculations have been performed in momentum space with the electromagnetic current treated in a fully covariant form and with the factorization assumption released;
2. our approach does not rely on the factorization approximation;
3. the agreement between the results of our calculations and the experimental data for both  $\phi = 0$  and  $\phi = \pi$ , is a very satisfactory one, particularly in view the lack of freely adjustable parameter in our approach;
4. the violation of the factorization approximation is appreciable at negative values of  $\mathbf{p}_m \geq 300 \text{ MeV}/c$ , whereas the non factorized and factorized results are in much better agreement in the whole range of positive values of  $\mathbf{p}_m$ ;
5. calculations of the 2bbu disintegration channel of  ${}^4\text{He}$ , i.e. the process  ${}^4\text{He}(e, e'p){}^3\text{H}$ , have already been performed [24] within the factorization approximation using realistic wave functions and taking exactly into account nucleon rescattering up to 3rd order. Calculations within a nonfactorized approach are in progress and will be reported elsewhere [25]; they should in principle yield results appreciably differing from the predictions based upon shell-model type four-body wave functions, thus allowing a study of NN correlations at densities comparable to the density of cold nuclei;
6. our results for  ${}^3\text{He}$  generally agree with the ones obtained in Ref. [5], so that it would appear that the problem of the treatment of FSI at high values of  $Q^2$  (or high  $\mathbf{p}_1$ ) is under control;

## V. ACKNOWLEDGMENTS

The authors are indebted to A. Kievsky for making available the variational three-body wave functions of the Pisa Group. Thanks are due to M.A. Braun for stimulating discussions on the Feynman diagram approach to nucleon rescattering and to S. Gilad, H. Morita, E. Piassetzky, M. Sargsian, R. Schiavilla and M. Strikman for many useful discussions concerning both the experimental and theoretical aspects of the topic considered in this paper. L.P.K. is indebted to the University of Perugia and INFN, Sezione di Perugia, for a grant and for warm hospitality.

- 
- [1] M. M. Rvachev et al., Phys. Rev. Lett. **94** (2005) 192302.
  - [2] F. Benmokhtar et al., Phys. Rev. Lett. **94** (2005) 082305.
  - [3] C.Ciofi degli Atti, L.P. Kaptari, Phys. Rev. **C71** (2005) 024005.
  - [4] C.Ciofi degli Atti, L.P. Kaptari, Phys. Rev. Lett. **95** (2005) 052502.
  - [5] R. Schiavilla, O. Benhar, A. Kievsky, L.E. Marcucci, M. Viviani, Phys. Rev. **C72** (2005) 064003.
  - [6] J.-M. Laget, Few-Body Systems Suppl. **15** (2003) 171; nucl-th/0303052.
  - [7] J.-M. Laget, Nucl. Phys. **A579** (1994) 333.
  - [8] J.-M. Laget, Phys. Rev. **C72** (2005) 024001.
  - [9] A. Kievsky, S. Rosati and M. Viviani, Nucl. Phys. **A551** (1993) 241 and *Private communication*.
  - [10] R. B. Wiringa, V. G. J. Stoks and R. Schiavilla, Phys. Rev. **C51** (1995) 38.
  - [11] L.L. Frankfurt, W.R. Greenberg, G.A. Miller, M.M. Sargsian, M.I. Strikman, Z. Phys. **A352** (1995) 97.
  - [12] V.N.Gribov, Sov. Phys. JETP, **30** (1970) 709.
  - [13] L. Bertocchi, Nuovo Cimento, **11A** (1972) 45.
  - [14] T. de Forest Jr., Nucl. Phys. **A392** (1983) 232.
  - [15] J. J. van Leeuwe *et al*, Phys. Lett. **B523** (2001) 6.
  - [16] S. Janssen, J. Ryckebusch, W. Van Nespén, D. Debruyne, Nucl. Phys. **A 672** (2000) 285.
  - [17] S. Boffi, C. Giusti and F.D. Pacati, Phys. Rep. **226** (1993) 1.

- [18] M.M. Sargsian, Int. J. Mod. Phys. **E10**(2001)405.
- [19] S. Jeschonnek, Phys. Rev. **C 63** (2001) 034609.
- [20] A. Bianconi, S. Jeschonnek, N. N. Nikolaev and B. G. Zakharov, Nucl. Phys. **A608** (1996) 437.
- [21] H. Morita, C.Ciofi degli Atti and D. Treleani, Phys. Rev. **C60**(1999) 34603-1.
- [22] S. Jeschonnek, T.W. Donnelly, Phys. Rev. **C57** (1998) 2438.
- [23] P.E. Ulmer, K.A. Aniol, H. Arenhövel, J,-P. Chen, *et al.*, Phys. Rev. Lett., **89** (2002) 062301-1.
- [24] H. Morita, M. Braun, C. Ciofi degli Atti, D. Treleani, Nucl. Phys. **A 699** (2002) 328
- [25] C.Ciofi degli Atti, L.P. Kaptari and H. Morita, *work in progress*.

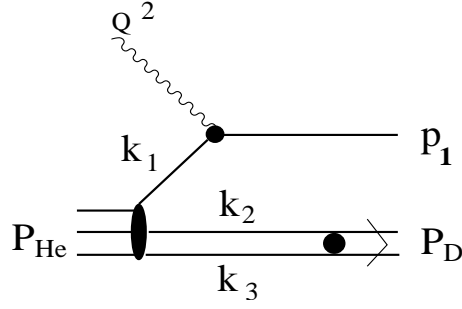


FIG. 1: The Feynman diagram for the the process  ${}^3\text{He}(e, e'p){}^2\text{H}$  in plane wave impulse approximation (PWIA).

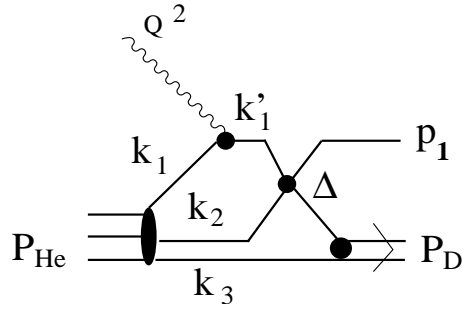


FIG. 2: Single rescattering diagram for the the process  ${}^3\text{He}(e, e'p){}^2\text{H}$ . The missing momentum  $\mathbf{p}_m$  is defined as  $\mathbf{p}_m = \mathbf{P}_D$ . The momentum of the active proton  $\mathbf{k}_1$  before the electromagnetic interaction satisfies the relation  $\mathbf{k}_1 = -(\mathbf{k}_2 + \mathbf{k}_3) = -\mathbf{p}_m + \Delta$

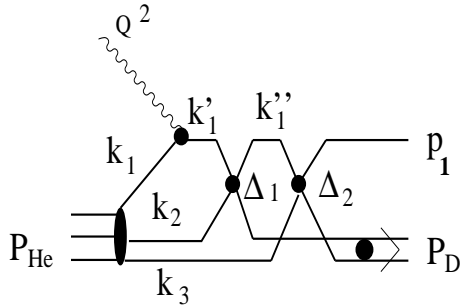


FIG. 3: Double rescattering diagram for the the process  ${}^3\text{He}(e, e'p){}^2\text{H}$ . The missing momentum  $\mathbf{p}_m$  is defined as  $\mathbf{p}_m = \mathbf{P}_D$ . The momentum of the active proton  $\mathbf{k}_1$  before the electromagnetic interaction satisfies the relation  $\mathbf{k}_1 = -(\mathbf{k}_2 + \mathbf{k}_3) = -\mathbf{p}_m + \Delta_1 + \Delta_2$

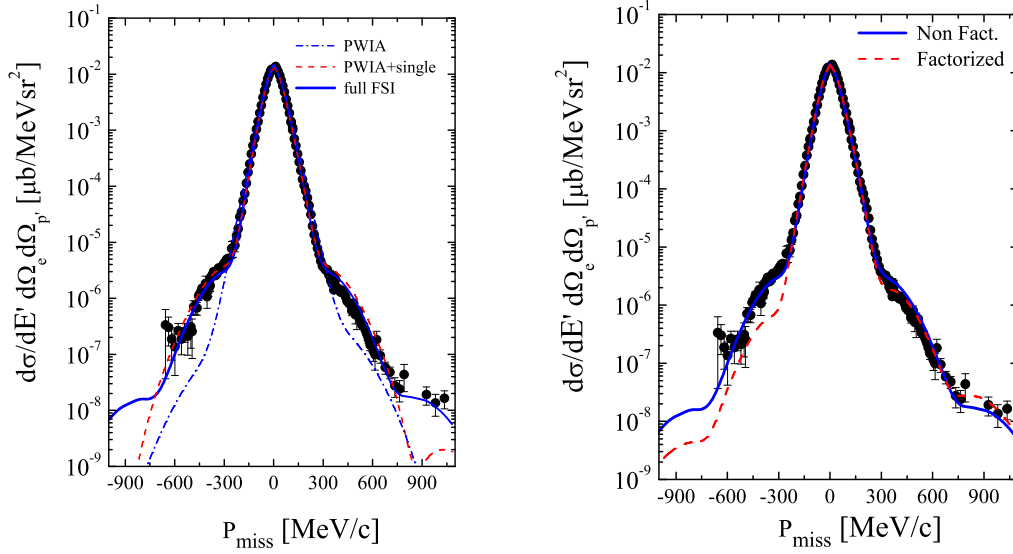


FIG. 4: The differential cross section for the process  ${}^3\text{He}(e, e'p)^2\text{H}$ . In the left panel the results of the non factorized calculations are shown. *Dot-dashed curve*: PWIA; *dashed curve* PWIA plus single rescattering FSI; *full curve*: PWIA plus single and double rescattering FSI. In the right panel the present non factorized results (*full curve*) are compared with the results obtained within the factorization (*dashed curve*). Experimental data from ref. [1]



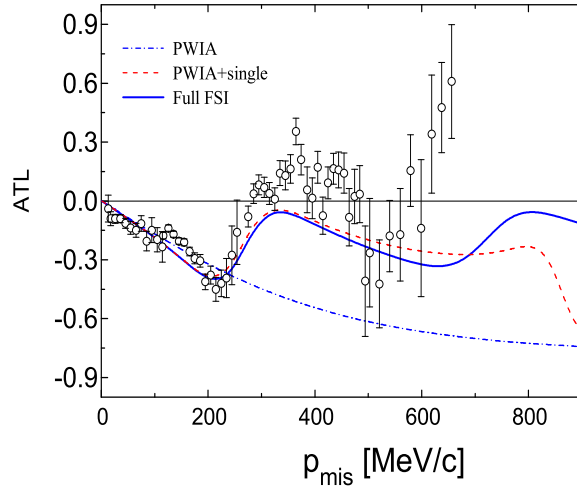


FIG. 5: The left-right asymmetry for the process  ${}^3\text{He}(e, e'p)^2\text{H}$ . *Dot-dashed curve*: PWIA; *dashed curve*: PWIA plus single rescattering FSI; *full curve*: PWIA plus single and double rescattering FSI. Experimental data are from ref. [1]

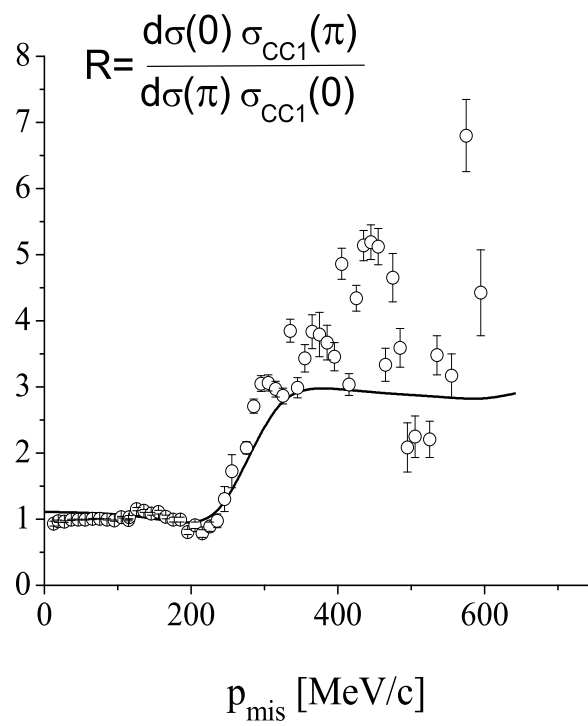


FIG. 6: The reduced ratio (25) obtained within the present approach (*curve line*) compared with the corresponding experimental data [1]